Monte Carlo studies of model Langmuir monolayers

S. B. Opps,* B. Yang,† C. G. Gray, and D. E. Sullivan
Department of Physics and Guelph-Waterloo Physics Institute, University of Guelph, Guelph, Ontario, Canada N1G 2W1
(Received 2 August 2000; revised manuscript received 14 November 2000; published 23 March 2001)

This paper examines some of the basic properties of a model Langmuir monolayer, consisting of surfactant molecules deposited onto a water subphase. The surfactants are modeled as rigid rods composed of a head and tail segment of diameters σ_{hh} and σ_{tt}, respectively. The tails consist of $n_t \approx 4-7$ effective monomers representing methylene groups. These rigid rods interact via site-site Lennard-Jones potentials with different interaction parameters for the tail-tail, head-tail, and head-head interactions. In a previous paper, we studied the ground-state properties of this system using a Landau approach. In the present paper, Monte Carlo simulations were performed in the canonical ensemble to elucidate the finite-temperature behavior of this system. Simulation techniques, incorporating a system of dynamic filters, allow us to decrease CPU time with negligible statistical error. This paper focuses on several of the key parameters, such as density, head-tail diameter mismatch, and chain length, responsible for driving transitions from uniformly tilted to untilted phases and between different tilt-ordered phases. Upon varying the density of the system, with $\sigma_{hh}=\sigma_{tt}$, we observe a transition from a tilted (NNN)-condensed phase to an untilted-liquid phase and, upon comparison with recent experiments with fatty acid-alcohol and fatty acid-ester mixtures [M. C. Shih, M. K. Durbin, A. Malik, P. Zschack, and P. Dutta, J. Chem. Phys. **101**, 9132 (1994); E. Teer, C. M. Knobler, C. Lautz, S. Wurlitzer, J. Kildae, and T. M. Fischer, J. Chem. Phys. **106**, 1913 (1997)], we identify this as the $L_2'/\mathrm{Ov}-L_1$ phase boundary. By varying the head-tail diameter ratio, we observe a *decrease* in T_c with increasing mismatch. However, as the chain length was increased we observed that the transition temperatures *increased* and differences in T_c due to head-tail diameter mismatch were diminished. In most of the present research, the water was treated as a hard surface, whereby the surfactants are only allowed to move within the plane of this surface. However, we have also utilized a more realistic model for the surfactant-water interactions, developed by Karaborni and Toxvaerd, in order to examine the role which the coupled effects of head group size and head group-subphase interactions plays in determining tilt ordering and on the stability of the monolayer. It is found that increasing the head diameter results in a widening of the air-water interface and an associated destruction of orientational order. Furthermore, the onset of capillary waves at lower temperatures for larger head diameters implies that the L_2-L_1 phase boundary for acids and acetates should move to lower temperatures relative to the $L_2'/\mathrm{Ov}-L_1$ phase boundary for alcohols and esters. This feature has yet to be seen in experimental studies.

DOI: 10.1103/PhysRevE.63.041602 PACS number(s): 68.35.Ct, 68.35.Rh

I. INTRODUCTION

In the last few years there has been a growing interest in the properties of Langmuir monolayers [1–12], which consist of surfactant molecules deposited on a water surface. The surfactants self-assemble at the air-water interface with the hydrophilic head groups in contact with the aqueous subphase while the hydrophobic hydrocarbon tails point away from the water. Despite their relatively simple composition, Langmuir monolayers have a rich phase diagram displaying a variety of different ordered phases, as shown in the generic phase diagram for fatty acids Fig. 1(a). In particular, within the ''liquid-condensed'' (LC) region, there exist three phases (S, CS, and LS) where the surfactant chains are on average untilted and, at lower pressures, there are four phases in which the chains are tilted toward either nearest neighbors (NN) (denoted L_2 and L_2'') or toward next-nearest neighbors (NNN) (denoted L_2' and Ov). For clarity, and to conform with modern terminology [2], we shall omit usage of the term liquid condensed and from now on refer to these two types of condensed phases as either tilted condensed or untilted condensed. It has been noted that this phase diagram is applicable to a number of chemically different Langmuir monolayers, which implies that some universal features of the surfactant-water system must be responsible for the presence of different tilt-ordered phases.

Although there has been considerable progress in our understanding of such general characteristics, there still remain a number of unresolved issues pertaining to structure and the orders of transitions in the generic phase diagram [2]. Additionally, this phase diagram is constantly being modified with the inclusion of new phases, such as the recently discovered intermediate-tilted I phase [4], a modulated-tilted phase [6], and the division of the L_2' phase into two phases with differing tilt angle [7,9]. From these findings, it is clear that the present phase diagram is incomplete. Furthermore, experiments by Shih *et al.* [10] and Teer *et al.* [11] have found that, whereas certain *n*-alkyl acetates and acids share similar phase diagrams, both having three tilted phases L_2, L_2', L_2'', the corresponding alcohols and esters demonstrate a collapse of the L_2 phase, refer to Fig. 1(b). The

*Chemical Physics Theory Group, Department of Chemistry, University of Toronto, Toronto, Ontario, Canada M5S 3H6.
†KLA-Tencor Corp., 160 Rio Robles, San Jose, CA 95132.

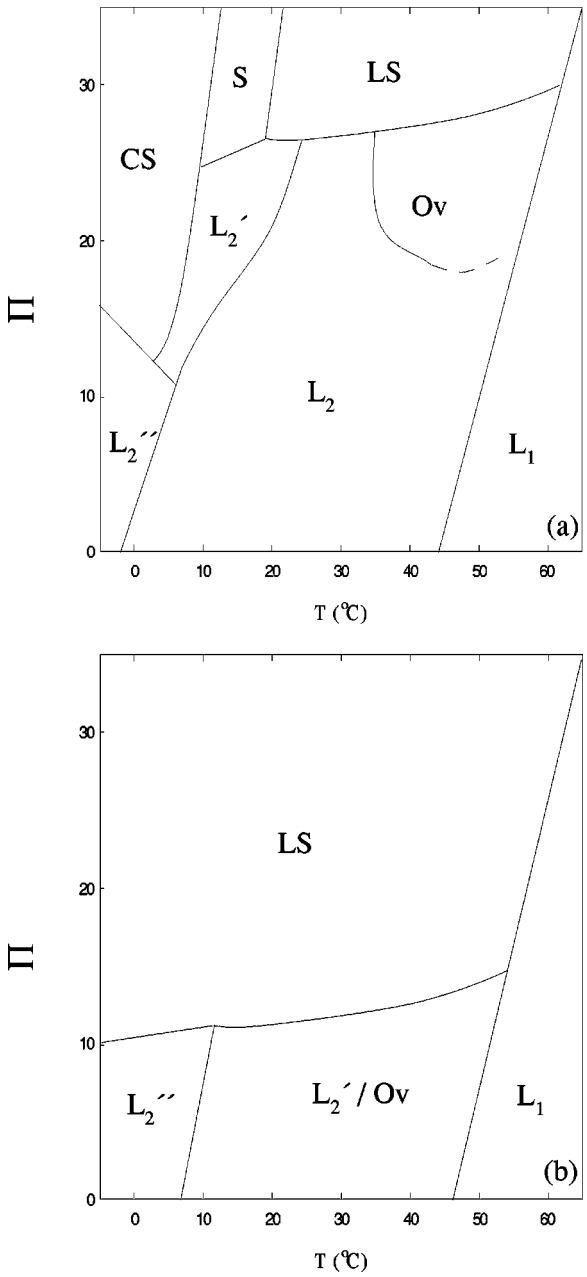

FIG. 1. Generic phase diagrams of surface pressure Π (in units of mN m^{-1}) versus temperature for Langmuir monolayers of (a) fatty acids or acetates and (b) alcohols or esters, displaying a variety of tilt-ordered, condensed phases in addition to the liquid (L_1) phase (adapted from Figs. 1 and 2(e) in Ref. [11]).

authors attribute these variations to differences in head size and head-substrate interactions, which would indicate that there *can be* fundamental differences in tilt ordering in the condensed phases due to the chemical structure of the surfactants. To examine such structural details, Stadler *et al.* [5] and Stadler and Schmid [6] have performed Monte Carlo simulations in the NΠT (constant molecular number, surface pressure and temperature) ensemble and mapped out the phase diagram for two different values of the head-tail diameter ratio.

In the present paper, we devise a simplified microscopic model for a Langmuir monolayer in order to gain a better understanding of their macroscopic properties. We have performed Monte Carlo simulations in the constant molecular number, area, and temperature (NAT) ensemble to examine the roles that several physical parameters, such as density and head-tail diameter mismatch, have in driving transitions from uniformly tilted to untilted phases. Some simulation techniques have been implemented to increase efficiency and minimize CPU time, including the construction of a system of dynamic filters. It has been found that the CPU time is reduced by 50% through the use of these filters.

To simplify the problem of characterizing the water subphase, in most of our studies that subphase has been replaced by a hard wall. Using this model, we first investigated the dependence of the tilting transition temperature T_c (between uniformly tilted and untilted phases) on the density of the system. Here the intent was to investigate the nature of the transition between the condensed and liquid phase. It has been argued [13] that such a transition cannot occur in a rigid rod system, and that the latter can only exhibit a solid to gas transition. However, we have found a transition from a tilted (NNN)-condensed to an untilted-liquid phase and, upon comparison with Fig. 1(b), we identify this as the L_2'/Ov $-L_1$ transition. Nonetheless, futher study over a greater density range is required to confirm the existence of such a transition and to obtain a more complete phase diagram.

In light of the recent experimental findings mentioned earlier, one of the primary objectives of this work was to examine the role of head-tail diameter mismatch on tilt ordering. By systematically varying the head-tail diameter ratio, we have observed a *decrease* in T_c with increasing mismatch, which is primarily an entropic effect. With greater mismatch between head and tail diameters, there is more available volume for the surfactant tails to undergo reorientation. The resultant increase in the orientational entropy tends to lower the critical temperature T_c. As the chain length was increased from $n_t=4$ to $n_t=7$, we observed that the transition temperatures increased, in agreement with experiment [1–3]. Additionally, the increased chain length tended to diminish differences in T_c due to head-tail diameter mismatch.

To improve upon the hard-wall model, we considered several other potential models to characterize the interactions between the surfactants and the water subphase. One of these was the (9-3) Lennard-Jones potential, but this was found to produce several unphysical results, such as premature collapse of the monolayer, as described later. To more accurately model these interactions, we considered the Fermi-like potential introduced by Toxvaerd and Karaborni [14,15]. Using the latter model, we have been able to replicate the staggering of the head groups across the water interface, as found in experiments [20,21] as well as molecular-dynamics studies [24]. We have also observed a substantial decrease in the mean tilt angle, $\langle\theta\rangle$, for the Fermi-like (FL) model compared to the hard surface (HS) model. Additionally, we have studied the coupled effects of head size and head-substrate interaction on the ordering and stability of the monolayer. We have found that an increase in head diameter leads to a widening of the air-water interface and an associated destruction

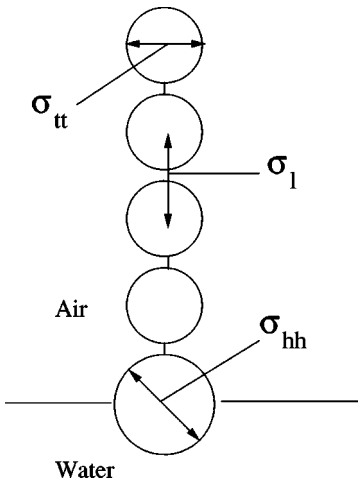

FIG. 2. A rigid coarse-grained model for surfactant molecules, characterized by bondlength σ_l, head diameter σ_{hh}, tail diameter σ_{tt}, and tail length, which depends on the number of effective monomers in the chain.

of orientational order. At higher temperatures capillary waves are exhibited, the onset of which occur at lower temperatures for larger head diameters. The destabilization of the monolayer for larger head diameters, where the tilting is in the nearest-neighbor (NN) direction, implies that the L_2-L_1 phase boundary should move to lower temperatures for acids and acetates [refer to Fig. 1(a)] relative to the L_2'/Ov $-L_1$ phase boundary for esters and alcohols [refer to Fig. 1(b)]. This property has yet to be examined in experimental studies.

The paper is organized as follows. In Sec. II we give an outline of the model and explanation for the choice of potentials. In Sec. III we discuss the details of how the Monte Carlo simulations are performed. The results from these simulations are presented in Sec. IV and conclusions are drawn in Sec. V.

II. MODEL

In a recent paper [9], we have described a coarse-grained model in which surfactants are treated as rigid rods composed of a head group, represented by a single effective monomer, and a tail containing n_t effective monomers, as illustrated in Fig. 2. Adjacent pairs of monomers (both tail tail and head tail) are separated by a bondlength denoted σ_l. Site-site interactions between monomers on different molecules are represented by (12-6) Lennard-Jones potentials of the form

$$U_{\alpha\beta}(r)=4\varepsilon_{\alpha\beta}\left[\left(\frac{\sigma_{\alpha\beta}}{r}\right)^{12}-\left(\frac{\sigma_{\alpha\beta}}{r}\right)^{6}\right], \tag{1}$$

where $\varepsilon_{\alpha\beta}$ and $\sigma_{\alpha\beta}$ are strength and range parameters, respectively, and the indices α,β label which types of sites (i.e., head h and/or tail t) are interacting. The parameters for interactions between different types of sites obey the conventional mixing rules, $\varepsilon_{\alpha\beta}=(\varepsilon_{\alpha\alpha}\varepsilon_{\beta\beta})^{1/2}$ and $\sigma_{\alpha\beta}=(\sigma_{\alpha\alpha}+\sigma_{\beta\beta})/2$. For computational efficiency, as usual in simulations, the Lennard-Jones potential between tail units $U_{tt}(r)$ was truncated at $r=2.5\sigma_{tt}$ and shifted in order to remain continuous. The head-head and head-tail potentials, $U_{hh}(r)$ and $U_{ht}(r)$, were truncated and shifted at their respective minima, $r_{\alpha\beta}^{\min}\equiv 2^{1/6}\sigma_{\alpha\beta}$, so that the latter interactions are treated as being purely repulsive.

The bulk of the work reported in this paper utilized an infinitely attractive hard wall to represent the surfactant-water interactions. In this sense, our research is comparable to that of Binder and co-workers [16–18]. With the hard-surface model, which we refer to from now on as HS, the molecules are grafted onto a rigid surface and only allowed to move within the plane of the wall, i.e., the head groups are not permitted to sink into the water or leave the water surface.

To more realistically model the surfactant-water interactions, we also considered a Lennard-Jones (9-3) potential, from here on referred to as the (9-3) model [19]. By allowing the surfactants to move both within the plane of the water surface as well as penetrate slightly into the water subphase, we hoped to replicate features found in experiments, such as staggering of the head groups across the air-water interface [20,21], as well as examine how these effects influence tilting behavior. The water subphase plays an important role in determining the ordering of the monolayer. Specifically, the acidity of the water can have a strong influence on the solubility of the surfactants in water and, in turn, affect the stability of the monolayer. Although the influence of pH has not been explicitly incorporated into the model, we attempted to approximate such effects by varying the strength of the interaction parameters.

For reasons noted previously by Harris and Rice [19], and confirmed by our own studies (see Sec. IV B 1), the (9-3) potential is not suitable and produces several defects, particularly ''collapse'' of the monolayer. Hence, we turned to a more realistic model introduced by Toxvaerd and Karaborni [14,15], which utilizes Fermi-like functions to characterize the water-surfactant interactions. This Fermi-like form, from here on referred to as the FL model, allows for better penetration of the water around the surfactant heads. In particular, Toxvaerd and Karaborni devised their model based upon solubility data of the head groups and methylene CH_2 groups. Instead of using a sharp wall to represent the air-water interface, continuous finite-width interfaces were employed, such that there is a net gain in energy when either head groups or tail segments pass from favorable to unfavorable regions. For the methylene tail segments, the continuous increase in energy in crossing from the air to water side of the interface is represented by the potential [14]

$$U_{wt}(z)=\begin{cases}\dfrac{\beta_1\varepsilon}{1+[1-(z/\alpha_1\sigma)]^{\tau_1}}, & z<\alpha_1\sigma\\ 0, & z\geqslant\alpha_1\sigma\end{cases} \tag{2}$$

where wt denotes the water-tail (methylene) interaction, $\varepsilon_{tt}\equiv\varepsilon=665$ J/mol is the interaction strength of the methylenes, and $\sigma_{tt}\equiv\sigma=3.527$ Å is the effective diameter of a methylene group. The parameter $\beta_1=8.27$ is used to control the

height of the potential barrier, which is proportional to the free energy of transfer of a methylene segment from a hydrocarbon to water, and the parameters $\alpha_1=6$ and $\tau_1=-32$ control the steepness of the potential. For the water-head group interaction, there is a continuous increase in energy in passing from the water to the air side of the interface so that the potential has the form,

$$U_{wh}(z)=\begin{cases}\dfrac{\beta_2\varepsilon}{1+[1-(z/\alpha_2\sigma)]^{\tau_2}}, & z>\alpha_2\sigma\\ 0, & z\leqslant\alpha_2\sigma\end{cases} \tag{3}$$

The parameters are determined in the same context as that for the water-tail interactions; $\beta_2=82.7$ is used to control the height of the potential barrier, which is proportional to the free energy of transfer of a head group from water to a hydrocarbon, and the other parameters were chosen as $\alpha_2=-6$ and $\tau_2=-16$.

III. SIMULATION DETAILS

All of our simulations were performed using the Metropolis Monte Carlo method in the canonical (NAT) ensemble. The simulation cell was based on an equilateral paralellogram in the plane of the water surface, taken to be the xy plane, with an angle of 60° between the sides, consistent with a close-packed triangular lattice. Periodic boundary conditions along two triangular directions in the xy plane were applied. For the HS model, the head groups were restricted to moving only within this plane, whereas for both the (9-3) and FL models of the aqueous subphase, the surfactants also could move perpendicular to the plane of the surface.

Most of our runs were initiated with $N_{\rm mol}=100$ molecules arranged in an untilted orientation on a regular triangular lattice. We define an effective reduced density as

$$\rho^*=\frac{\rho}{\rho_{cp}}, \tag{4}$$

where $\rho\equiv N_{\rm mol}/A$ is the number of molecules per area A and the close-packed density is taken to be

$$\rho_{cp}=\left[\frac{\sqrt{3}}{2}(r_{hh}^{\rm min})^2\right]^{-1}, \tag{5}$$

corresponding to an assumed optimal hexagonal packing of the head groups at the minimum of the Lennard-Jones potential, with $r_{hh}^{\rm min}=2^{1/6}\sigma_{hh}$. In the following results, temperature is expressed in the reduced unit $T^*=k_BT/\varepsilon_{tt}$.

A. Thermalization and averages

A typical simulation in our paper involves 2×10^6 Monte Carlo sweeps (MCS), where a single sweep consists of $N_{\rm mol}$ trials (i.e., one trial per molecule), with initial thermalization periods on the order of 250 000 MCS. In general, simulations at low temperatures or in the vicinity of critical points are run for twice the length of time of other simulations. Once the system has equilibrated, ensemble averages of the thermodynamic quantities of interest are calculated over the remaining MCS. Since we are making single-particle moves, neighboring sample states are expected to be highly correlated and *not* independent. To sample only independent states requires an estimate of the correlation ''time'' in our simulations, which was achieved using a binary bining algorithm developed by Belohorec and Nickel [22]. Using this, we have determined that the correlation time for our system is ~500 MCS and mainly insensitive to the thermodynamic state.

B. Filtration

In addition to a number of standard methods by which to improve the efficiency of a simulation, we have developed a ''filtration'' scheme that dramatically reduces the CPU time. A full description of these filters is provided in Ref. [23].

At a given trial move for molecule k, one is first required to establish a new neighbor list for k. For a particular molecule l to ''qualify'' as a neighbor, the separation between its head and k's head must lie within a certain maximum distance $R^{\rm max}$ (here we consider the model where the molecules are not allowed to leave the substrate surface). This distance is calculated at the beginning of the simulation and is dependent on the size of the simulation box, the density of molecules, and the length of the surfactant tails. For purely atomic systems, it would be sufficient to establish a cutoff at $\sim3.0\sigma_{hh}$. However, for the monolayer system, one must be careful not to omit potential overlap between monomers on widely separated surfactant tails, which could occur at low densities. A typical cutoff value for our simulations ranges between 3 and $6\sigma_{hh}$.

Upon calculating the site-site distance r between two monomers on molecules k and l, it might be found that $r^2\ll\sigma^2$, i.e., the interaction potential between the monomers is strongly repulsive. It is perfectly valid to proceed and calculate all of the remaining site-site distances and energies, but this might be a considerable waste of effort. If r^2 is less than some threshold value $d_{\rm min}^2$, corresponding to approximately infinite hard-core repulsion, then the resulting very large positive energy will dominate all other site-site interactions and it is probable that the trial move for molecule k will fail the Metropolis acceptance criterion. As such, we could immediately exit the energy calculations for that trial and attempt a new move. This first line of ''filtration'' greatly improves the speed of a simulation and does not affect the physics, as long as one is careful to select $d_{\rm min}$ such that the interactions are sufficiently repulsive.

For $r^2>d_{\rm min}^2$, we are required to proceed with the energy calculation. However, a second level of filtration can be implemented to decrease the CPU time of this calculation, with minimal statistical error, as follows. Having made a trial move for molecule k, in principle one should calculate the new energy of the system, denoted U_j. If the energy of the system before the trial was U_i, then the move would be accepted with probability $\min[1,\exp(-\beta\Delta U_{ij})]$, where $\Delta U_{ij}\equiv U_j-U_i$, under the standard Metropolis scheme. Note that if

$$\Delta U_{ij} > U^*, \tag{6}$$

where $U^* > 0$ is some threshold value, this will have very small Boltzmann weighting (i.e., low probability) and will almost always be rejected.

To establish U^*, one needs some knowledge about the magnitude of repulsive energies required so that the acceptance/rejection ratios obtained using the filtering condition [Eq. (6)] do not depart significantly from the ratios obtained without applying the filter. This is readily obtained by monitoring the energies and acceptance ratios for the thermalization stage of a simulation (without filters present). It is advantageous to begin from a random configuration of molecules, since this will generate a large number of molecular overlaps. For the present system, we have determined that a threshold value of $U^* \sim 10 k_B T$ is sufficient to guarantee the proper functioning of the filter.

If at some neighbor l it is found that the interaction energy between k and l is $> U^*$, then it might be possible to exit the energy calculation *before* calculating the interactions between k and all of its remaining neighbors. However, this would require one to know *a priori* that the sum of all of the other neighbor interactions is not sufficiently negative so as to reduce the total energy below the threshold. Instead of actually calculating this energy, we can derive a lower bound estimate based on the most optimal packing configuration (analogous to an approximate ground-state calculation), $U_{\min}(l)$. The index l indicates that the energy estimate corresponds to the lower bound contribution from the remaining $l+1$ to N_{nbr} neighbors in the neighbor list of molecule k. Hence, for each neighbor that we pass in the list, the estimate decreases and is, in this sense, *dynamic*. The details of how these estimates are derived are discussed in Ref. [23].

Note that by implementing these filters, it is computationally cheaper to reject a move than to accept it. To accommodate for this mismatch (or take advantage of it), one can make larger molecular displacements (both translational and orientational) resulting in a lower acceptance ratio than the standard 50%, which may be closer to $30-40\,\%$. The filter scheme becomes very important at lower temperatures where the system is more prone to falling into local free energy minima. With the use of these dynamic filters, we have achieved a 50% increase in speed with negligible statistical error.

IV. RESULTS AND ANALYSIS

One of the main objectives of our work was to investigate the effects on tilting transitions resulting from variations in the head-tail diameter mismatch. For all of the following work, we have fixed the relative values of the strength parameters to be $\varepsilon_{tt} = 0.72 \varepsilon_{hh}$ and the bondlength $\sigma_l = 0.7 \sigma_{tt}$. These values scale according to those used in the molecular dynamics study by Karaborni and Toxvaerd [15].

In order to study tilting transitions, one needs to determine appropriate measures of the tilt order. We have used the dimensionless order parameter introduced by Haas *et al.* [18],

$$R_{xy} = \langle \overline{e_x}^2 + \overline{e_y}^2 \rangle^{1/2}, \tag{7}$$

where

$$\overline{e_x} = \frac{1}{N_{\text{mol}}} \sum_{j=1}^{N_{\text{mol}}} e_{j,x}, \tag{8}$$

and where $\mathbf{e}_j$ is the unit vector along the molecular axis of molecule j. R_{xy} is a measure of the in-plane azimuthal ordering of the projections of the molecular axes. In a uniform tilt-ordered phase, with a hexagonal lattice structure, there are six equivalent directions for in-plane ordering of the molecular axes, and simulation configurations could contain a ''mixture'' of these different directions. The order parameter R_{xy} has the advantageous feature of being independent of these tilt directions and has the property that it is $\mathcal{O}(1)$ in the ordered phase and $\mathcal{O}(1/\sqrt{N_{\text{mol}}})$ in the disordered phase. Another relevant measure of the order is the mean tilt angle $\langle \theta \rangle$,

$$\langle \theta \rangle = \left\langle \frac{1}{N_{\text{mol}}} \sum_{j=1}^{N_{\text{mol}}} \theta_j \right\rangle, \tag{9}$$

where θ_j is the polar angle between $\mathbf{e}_j$ and the z axis. This order parameter should decrease in the disordered phase but not approach zero since θ_j is a positive definite quantity.

In addition to the tilt-order parameters, which provide information about the orientational ordering in the system, we have also examined the structure factor, defined as

$$S_{\mathbf{k}} = \frac{1}{N_{\text{mol}}} \left\langle \sum_{i,j}^{N_{\text{mol}}} e^{i\mathbf{k}\cdot(\mathbf{r}_i - \mathbf{r}_j)} \right\rangle - N_{\text{mol}} \delta_{\mathbf{k},0}, \tag{10}$$

where the double sum is over the positions $\mathbf{r}$ of all surfactant head groups, $\mathbf{k} = (k_x, k_y)$ is the scattering wave vector, and $\delta_{\mathbf{k},0}$ is the Kronecker delta. This allows us to monitor the positional order of the head groups in the plane of the water surface. At low temperatures, these head groups remain locked into a solidlike structure. As the temperature is increased, the system enters a liquidlike phase in which the head groups become disordered.

Besides the order parameters defined above, we have also monitored standard thermodynamic quantities such as the mean potential energy $\langle U \rangle$, surface pressure Π, and heat capacity C_v. The surface pressure is defined as,

$$\Pi = \gamma_w - \gamma_{ws}, \tag{11}$$

where γ_w is the surface tension for pure water and γ_{ws} is the surface tension of the combined surfactant-water system. For the models considered in this paper, where the aqueous subphase is represented by an external field, we can define $\gamma_w = 0$ and thus consider $\gamma_{ws} \equiv \gamma$ as the surface tension due to interactions involving surfactants. An expression for the surface tension can be derived from the thermodynamic relationship,

$$\gamma = \left(\frac{\partial F}{\partial A} \right)_{V,T}, \tag{12}$$

where F is the Helmholtz free energy, A is the area and the derivative is taken at fixed volume V and fixed temperature T. From this definition, one obtains the surface pressure as

$$\Pi = \frac{1}{A}\left\langle \frac{1}{2}\sum_{i<j}^{N_{\mathrm{mol}}} (3z_{ij}\hat{\mathbf{k}} - \mathbf{r}_{ij}) \cdot \sum_{\alpha,\beta}^{n} \hat{\mathbf{r}}_{\alpha\beta}^{ij} \frac{dU_{\alpha\beta}(r_{\alpha\beta}^{ij})}{dr_{\alpha\beta}^{ij}} + \sum_{i=1}^{N_{\mathrm{mol}}} z_i \sum_{\alpha=1}^{n} \frac{dU_{w\alpha}(z_\alpha^i)}{dz_\alpha^i} \right\rangle. \quad (13)$$

The indices i and j label different molecules whereas the indices α and β label monomers on the different molecules. Here $n = n_t + 1$ is the total number of monomers per molecule, $\mathbf{r}_{ij} = \mathbf{r}_j - \mathbf{r}_i$, where $\mathbf{r}_i$ is the position of the head group of molecule i, $\hat{\mathbf{k}}$ is the unit vector in the z-direction, and $\hat{\mathbf{r}}_{\alpha\beta}^{ij}$ denotes the unit vector pointing from site α on molecule i to site β on molecule j. It is not clear whether Eq. (13) agrees with that used by Karaborni and Toxvaerd [14], since the latter is expressed in a form that is strictly applicable only to monatomic liquids. In the case of the HS model, the term involving derivatives of the wall-site potentials $U_{w\alpha}(z)$ yield the ideal-gas contibution $k_B T N_{\mathrm{mol}}/A$ to Π while one can set $z_{ij} = 0$ in the term containing pair interactions.

A. Hard surface model

1. Variations in density

To compare with the generic phase diagram Fig. 1 for Langmuir monolayers, we first studied tilting behavior at different densities with $\sigma_{tt} = \sigma_{hh}$. Note that all of the observed tilted phases corresponded to tilting in the NNN direction. In Figs. 3(a) and 3(b), we display the tilt-order parameters at a number of different densities with $\sigma_{tt} = \sigma_{hh}$, and a tail length of $n_t = 4$. In this figure, the tilted-untilted critical temperature T_c is identified with the temperature at which the curves of $\langle \theta \rangle$ and R_{xy} vs T^* begin to level off. These are somewhat rough estimates since the curves broaden due to thermal fluctuations with increasing T and some of the curves have not yet completely flattened out. Nonetheless, one observes that T_c decreases with decreasing density, although there is an intermediate regime (for densities ranging between $\rho^* = 0.85$ and $\rho^* = 0.95$) where there does not appear to be any strong correlation between density and T_c. Such behavior suggests that this regime is within the tilted (NNN) condensed-untilted liquid coexistence region.

To further examine this hypothesis, we also calculated the surface pressure as a function of temperature, for the same range of densities. The corresponding phase diagram of the surface pressure versus temperature is given in Fig. 4. Comparison with Fig. 1(b) for Langmuir monolayers of esters (or alcohols), where the effective head diameter is smaller than that for the acids and acetates, supports identifying the curve displayed in Fig. 4 with the $L_2'/\mathrm{Ov} - L_1$ phase boundary, confirming our earlier hypothesis. However, there is debate about the existence of such a transition for rigid rods. In particular, it was concluded by Schmid [13] that neither stable tilted-condensed phases nor liquid phases can be found for rigid rods and there exists only a first-order phase

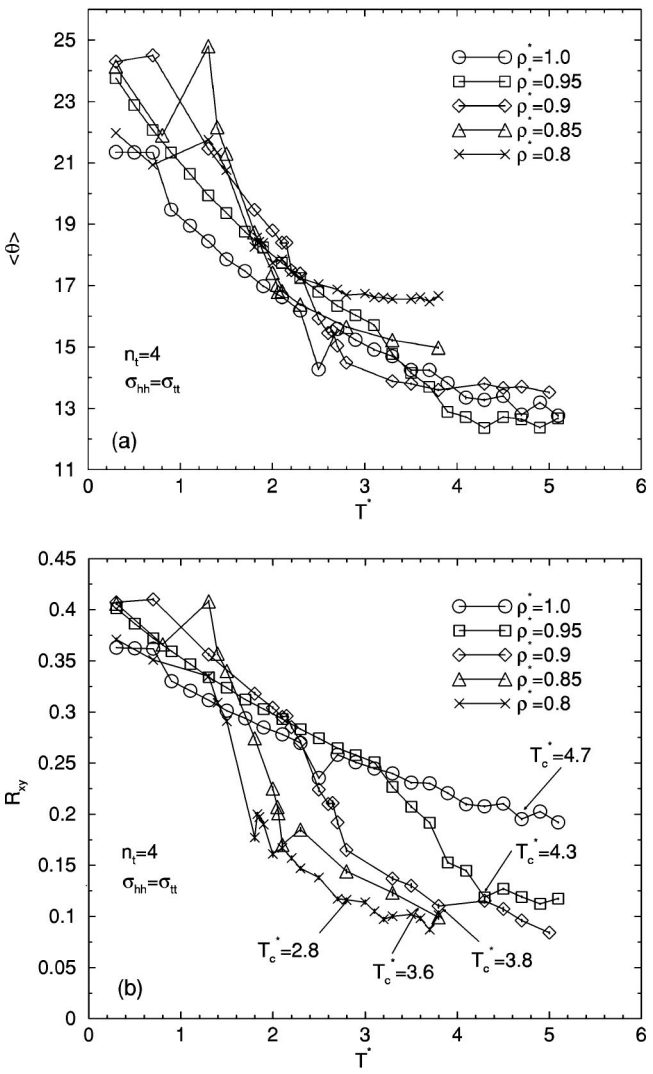

FIG. 3. Effects on tilting transitions due to variations in density, for $\sigma_{hh}/\sigma_{tt} = 1$ and $n_t = 4$: mean tilt angle $\langle \theta \rangle$ (degrees) (a), tilt order parameter R_{xy} (b), vs reduced temperature T^*.

transition between the gas phase and an untilted condensed phase. According to the mean-field theory in Ref. [13], chain flexibility is required to stabilize homogeneous tilted phases allowing for coexistence between the liquid phase and a tilted-condensed phase. In order to convincingly support or refute these arguments, a greater density range needs to be explored to properly map out the phase diagram and determine the stability of the tilted phases found in our paper.

2. Head-tail diameter mismatch

One of the primary motivations for examining the effects due to head-tail diameter mismatch has been the recent experimental findings [11] showing variations in tilt ordering due to differences in head diameter. As was shown in Ref. [8,9], increasing the head diameter drives a transition from the NNN to the NN tilted phase, which is consistent with these experiments [11]. We now consider the tilt-ordering behavior at finite temperature as a function of head diameter σ_{hh}. The following simulation results are performed at a

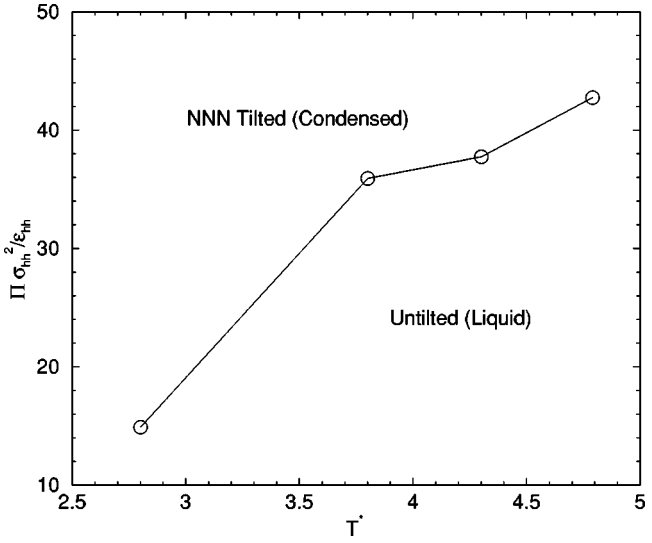

FIG. 4. Phase diagram of the surface pressure Π versus reduced temperature T^*, for the same states as in Fig. 3.

reduced density of $\rho^*=1.0$ with tails of fixed diameter σ_{tt} and of lengths $n_t=4$ and $n_t=7$.

In Figs. 5(a)–5(f), equilibrium configurations and structure factors are displayed for $n_t=7$ and $\sigma_{hh}=1.10\sigma_{tt}$ at reduced temperatures $T^*\equiv k_BT/\varepsilon_{tt}=0.97$, 3.75, and 9.03. It is clear that at low temperatures ($T^*=0.97$), the system is in a solidlike state as evident by the scattering peaks in the structure factor [Fig. 5(b)] corresponding to the reciprocal lattice of a centered rectangular lattice. The distortion of the hexagonal lattice, which is due to tilting in the NN direction, corresponds to contraction in the y direction and expansion in the x direction. This configuration is more clearly illustrated by the projections of the molecular axes in the xy plane, as shown in Fig. 5(a). Notice that the contraction in the y direction affords more optimal packing of parallel strips of tilted tails. Furthermore, one observes a number of dislocations, which result from the incommensurate structures of the head-group lattice and the simulation box. Another interesting and possibly related feature is that the head-group lattice is rotated slightly from the x axis by an amount of 4–5 degrees. At a temperature of $T^*=3.75$ [Figs. 5(c) and 5(d)], the tilting is still in the NN direction, with some tilting in a direction intermediate (I) between the NN and NNN directions, but the head-group lattice has rotated by $\sim -20°$ to $345°$, as seen in Fig. 5(c). At a temperature of $T^*\approx 4.31$, the system begins to become disordered and has become translationally disordered by $T^*=9.03$ [see Fig. 5(f)], although there still is some orientational ordering as seen in Fig. 5(e). In contrast, we have found that for tail length $n_t=4$, changes in the azimuthal direction of tilt ordering are almost immediately followed on further increase in temperature by a transition to an untilted disordered state. Therefore, for longer chains, translational disordering of the head-group positions occurs at significantly lower temperatures than orientational disordering of the chains.

To corroborate the above findings, we present heat capacity data for $n_t=7$ and several values of the head-diameter

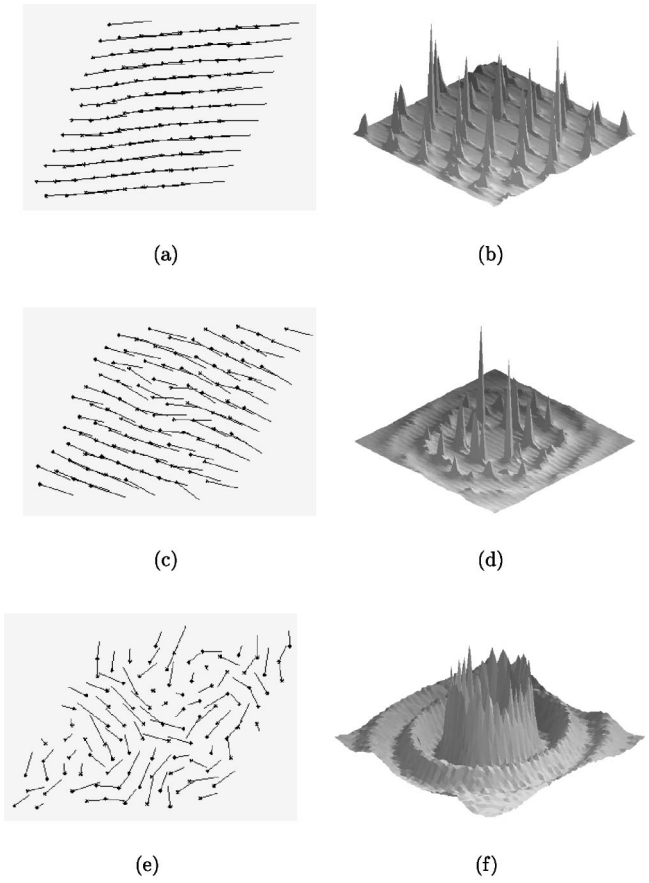

FIG. 5. Projections of the molecular axes in the xy plane and structure factors for $\sigma_{hh}/\sigma_{tt}=1.10$, $n_t=7$, and density $\rho^*=1.0$ at (a),(b) $T^*=0.97$; (c),(d) $T^*=3.75$; (e),(f) $T^*=9.03$.

tail-diameter ratio σ_{hh}/σ_{tt} in Fig. 6. The prominent peak in the heat capacity for $\sigma_{hh}/\sigma_{tt}=1.10$ and 1.20 corresponds to the onset of translational disordering. For $\sigma_{hh}/\sigma_{tt}=1.05$, there are two dominant peaks; the first peak, occuring at low

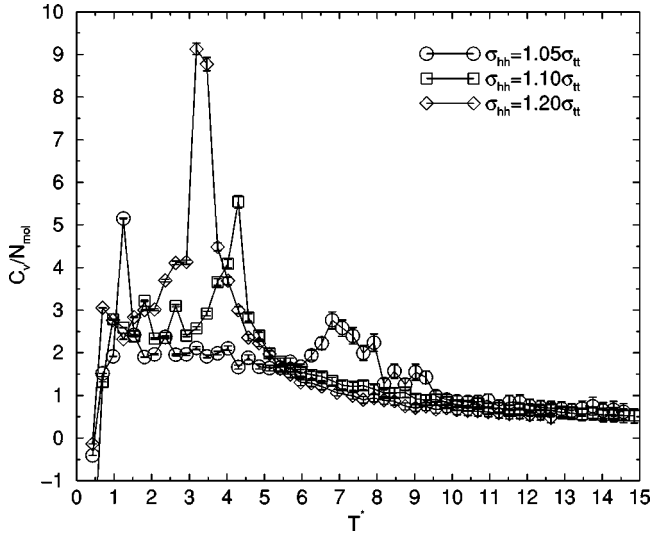

FIG. 6. Heat capacity per molecule (in units of k_B^{-1}) versus reduced temperature T^*, for various head-tail diameter ratios, at $n_t=7$ and density $\rho^*=1.0$.

temperature, is associated with distortions of the head-group lattice accompanied by a transition from NN to NNN tilting, and the second peak, at higher temperature, signals the disordering transition. In addition to the principal peaks, one also observes other features in the heat-capacity data. For $\sigma_{hh}=1.10\sigma_{tt}$, the series of smaller peaks preceding the main peak are not associated with transitions in tilt-ordering direction but are related to rotations of the head-group lattice, as we have discussed above. We have determined that, for temperatures below the disordering transition, the tilt is on average in the NN direction for $\sigma_{hh}/\sigma_{tt}=1.10$ and 1.20 and in the NNN direction for $\sigma_{hh}=1.05\sigma_{tt}$. Tilt-ordering transitions are observed at higher temperatures but these appear to be coupled to the translational disordering of the head groups. However, as mentioned above, there is still some orientational order in the system at temperatures substantially greater than that for translational disordering. One of the main differences between the heat-capacity data for $n_t=4$ and $n_t=7$ is that the second peak is shifted to higher temperatures for $n_t=7$, again showing that the onset of tilt disordering of the chains occurs at higher temperatures for longer chains.

To examine the tilt ordering in more detail, we show the mean tilt angle and tilt-order parameter R_{xy} for $n_t=4$ in Figs. 7(a) and 7(b). One observes that there is a decrease in the critical temperature as the head diameter is increased. This is an entropic effect resulting from a greater free volume available for the tails as the head-tail diameter ratio is increased. At low temperatures, the head-tail diameter mismatch favors tilting. This is an energetic effect and, again, is consistent with the results obtained from the ground-state analysis of Ref. [9]. As the temperature is increased, there is a competition between the energetic benefits of tilt ordering and the gain in entropy when the tails are, on average, untilted. Again, at higher temperatures the increase in the head-tail diameter ratio contributes to greater entropy of the chains and, thereby, tends to decrease the critical temperature.

For tails of length $n_t=7$, the mean tilt angle and tilt-order parameter are presented in Figs. 8(a) and 8(b). Although for longer chains it is more difficult to ascertain the exact location of T_c, since the levelling out of the curves occurs at substantially higher temperatures, we again see similar trends to those observed for $n_t=4$. In particular, T_c decreases with increasing head-tail diameter mismatch. However, one sees that the longer tail length $n_t=7$ results in larger values of T_c, in agreement with other simulation studies [6,16] and confirmed by experiment [1–3], and diminishes the differences in T_c due to increasing diameter mismatch.

Therefore, we conclude that increasing the tail length n_t tends to stabilize uniformly tilted phases and diminish the effects of head-tail diameter mismatch.

B. Water models

In the previous sections we reported our results for simulations performed on a HS model. As mentioned in Sec. II, we have also considered other models, namely, the (9-3) and FL models, which account approximately for more details of the water-surfactant interactions. This work was motivated by the observation that, as discussed in Ref. [11], it is the head-group-water interactions that govern the effective diameter of the head group and, in turn, influence the direction of tilt. In particular, it was argued that the collapse of the L_2 (NN) phase for alcohols and esters is a consequence of conformational changes of the head groups when they are in contact with water. Since we are using only a crude model for our head groups, we are unable to replicate such conformational changes. Nonetheless, it is instructive to analyze the effects due to variations in head diameter when head-group-water interactions are explicitly included in the model.

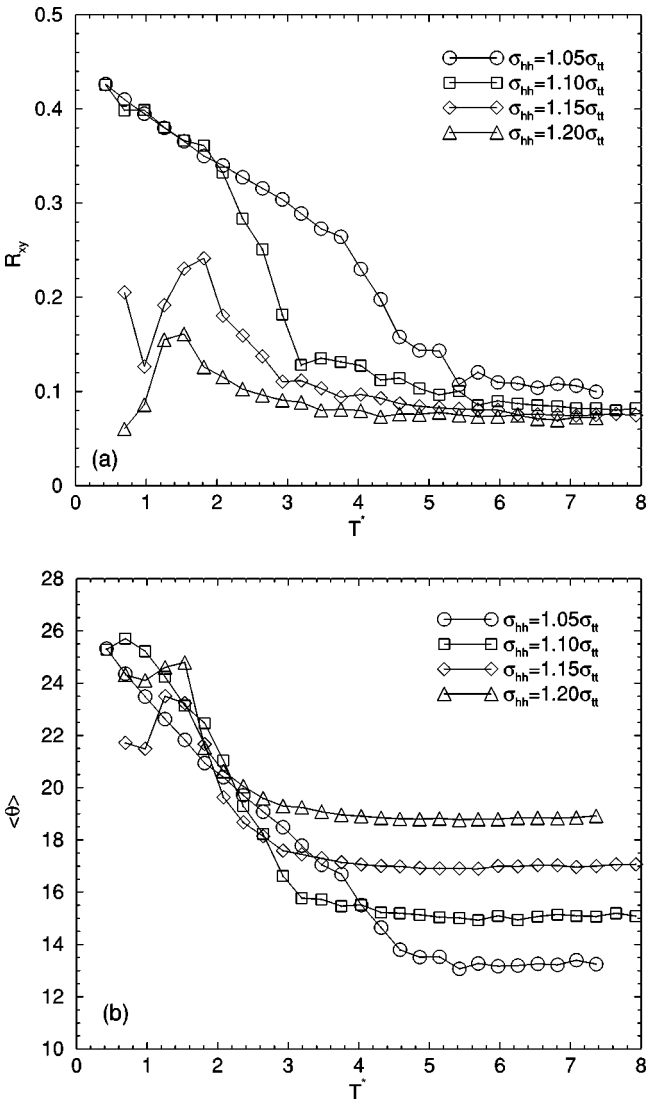

FIG. 7. Tilt-order parameter R_{xy} (a), and mean tilt angle $\langle\theta\rangle$ (b), vs reduced temperature T^*, for $n_t=4$, $\rho^*=1.0$, and indicated diameter ratios.

1. (9-3) Model

Here we briefly discuss the model where the water subphase is treated as a continuum and the interactions between surfactants and water substrate are governed by (9-3) potentials [19]. For the surfactant-surfactant interaction strengths and lengths, we used the values given by Karaborni and Tox-

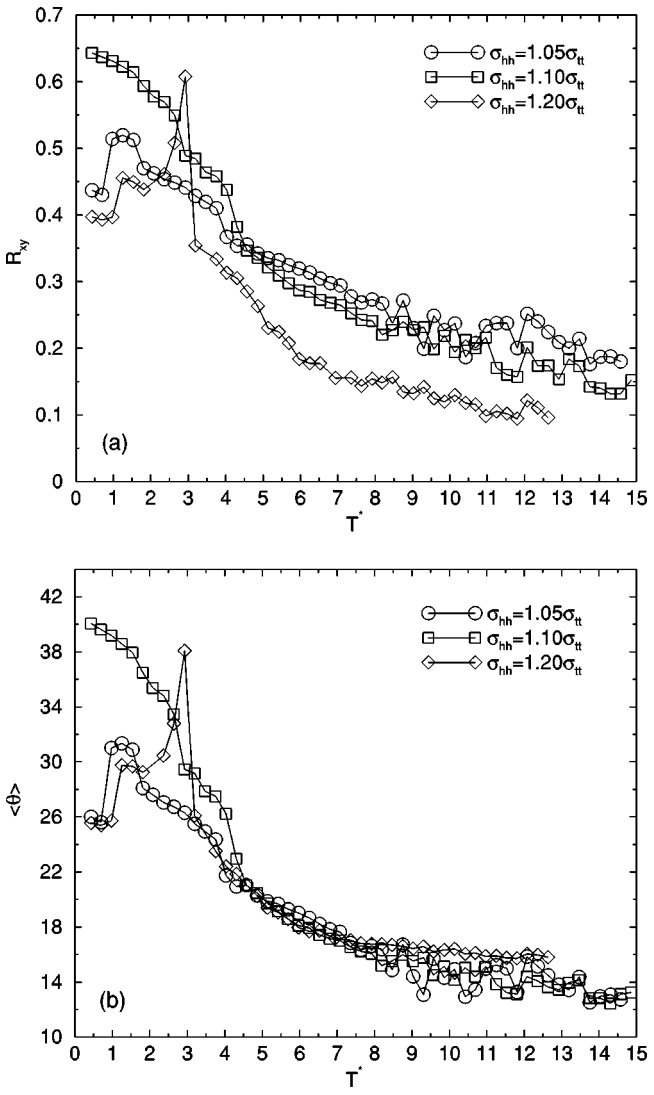

FIG. 8. Tilt-order parameter R_{xy} (a), and mean tilt angle $\langle\theta\rangle$ (b), vs reduced temperature T^*, for $n_t=7$, $\rho^*=1.0$, and indicated diameter ratios.

vaerd [15] and for the surfactant-water interactions, we used the parameters provided by Harris and Rice [19]. In agreement with the findings by Harris and Rice [19], we observed that at temperatures between 300 and 400 K the head groups begin separating from the water surface and the chains become inverted.

At slightly higher temperatures, about 1/3 of the molecules are removed from the water subphase and the system enters a gaseous state. The apparent lack of a liquid phase is also in accord with the results in Ref. [19]. In the latter work, the absence of the liquid phase was attributed to deficiencies in the model and an inadequate characterization of the water molecules and head groups.

It is clear that the 9-3 potential is too soft, since, in the vicinity of the minimum of the potential, moderate changes in z result in only minimal changes in the energy. This results in premature dissociation of head groups from the water surface. In particular, at moderate temperatures, the head groups can become delocalized from the surface with a considerable gain in entropy and only a minimal penalty in energy. Once the chains have inverted, it is too costly to rotate back to the original, lower-energy configuration. At higher temperatures, it is more favorable for the chains to enter the gas phase.

2. Fermi-like model

To model the surfactant-water interactions more realistically, we adopted the potentials used by Karaborni and Toxvaerd [14,15], described in Sec. II. In particular, this model allows the head groups to penetrate below the water surface, which is more realistic. Although the hydrocarbon tails on surfactants are hydrophobic, the interactions between the tails and water are not infinitely repulsive and the FL model accounts for this property. In our preliminary analysis using this model, we have studied the effects of varying head diameter on both the tilt ordering of the system and the stability of the monolayer. Using tails of length $n_t=7$ at a density of $\rho^*=1.12$ and bond length of $\sigma_l=0.7\sigma_{tt}$, we have performed simulations at temperatures of $T^*=1.39$ and 4.44. In the following figures we display equilibrium configurations and probability distributions for the z displacement of the head groups at $\sigma_{hh}=1.10\sigma_{tt}$ [Figs. 9(a) and 9(c)] and $\sigma_{hh}=1.20\sigma_{tt}$ [Figs. 10(a)–10(c)].

It can be seen in these figures that, even at low temperatures, the head groups are staggered across the water interface, which more accurately portrays the behavior of real monolayers. The width of the probability distribution for the z displacement gives a measure of the interface width created by the head groups. At higher temperatures, the interface widens, as indicated by the broadening of the probability distributions. Referring to the configuration figures, one also notices the development of surface waves as the system becomes disordered. The onset of the disordered phase occurs at temperatures substantially lower than those found for the hard surface model for $n_t=7$ in Sec. IV A 2. This is clearly because the presence of the water subphase allows for greater mobility of the chains and, hence, an increase in configurational entropy.

Comparing the z distributions corresponding to the different head diameters, at $T^*=1.39$, it is seen that the distribution is wider for the $\sigma_{hh}=1.20\sigma_{tt}$ case. This is indicated quantitatively by the standard deviation in z, values of which are given in Table I, along with values of the mean z displacement, which is also seen to be lower for larger head diameter. These results can be attributed to the fact that, for larger head diameters, the head groups must form a more staggered structure in order to maintain optimal packing of the chains. As we have noted, the interface width increases with increasing temperature. Furthermore, it appears that increased tail-head diameter mismatch tends to compound the disordering effect due to the presence of water.

In terms of the tilt ordering of the system, we find similar trends to those determined in Sec. IV A 2. In particular, the tilted states corresponding to smaller head-tail diameter mismatch, remain stable to higher temperatures than for larger mismatch. It is found that, at $T^*=1.39$, the tilt is in the NNN direction for $\sigma_{hh}=1.10\sigma_{tt}$, whereas the tilt is in the I and NN directions for $\sigma_{hh}=1.20\sigma_{tt}$. Additionally, one of the

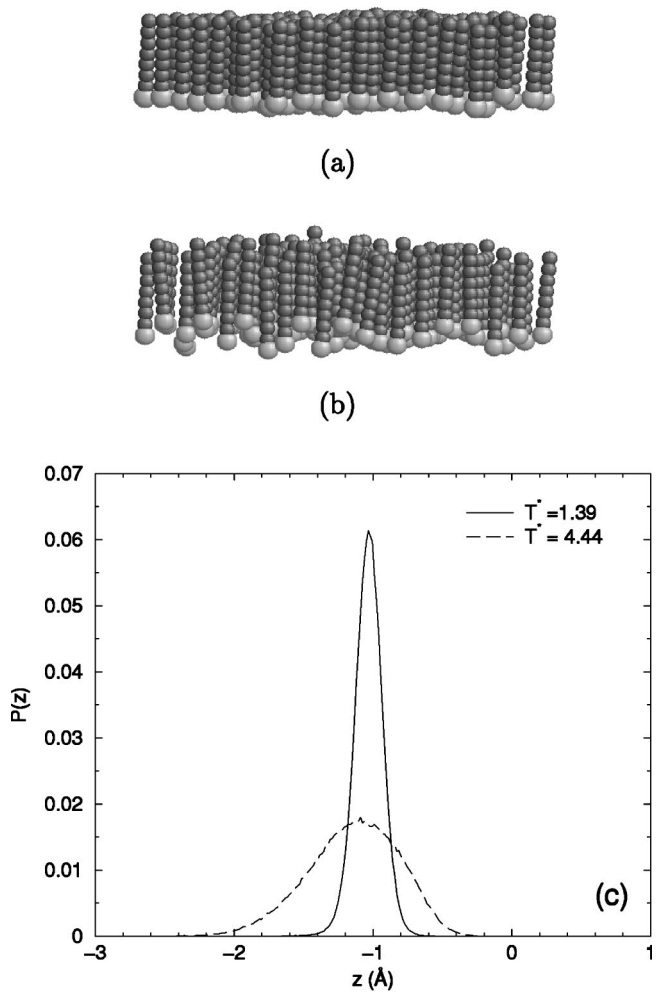

FIG. 9. Equilibrium configurations using the FL model at $\rho^* = 1.12$, $n_t = 7$, for $\sigma_{hh} = 1.10\sigma_{tt}$: (a) $T^* = 1.39$, (b) $T^* = 4.44$, (c) corresponding z displacement probability distributions.

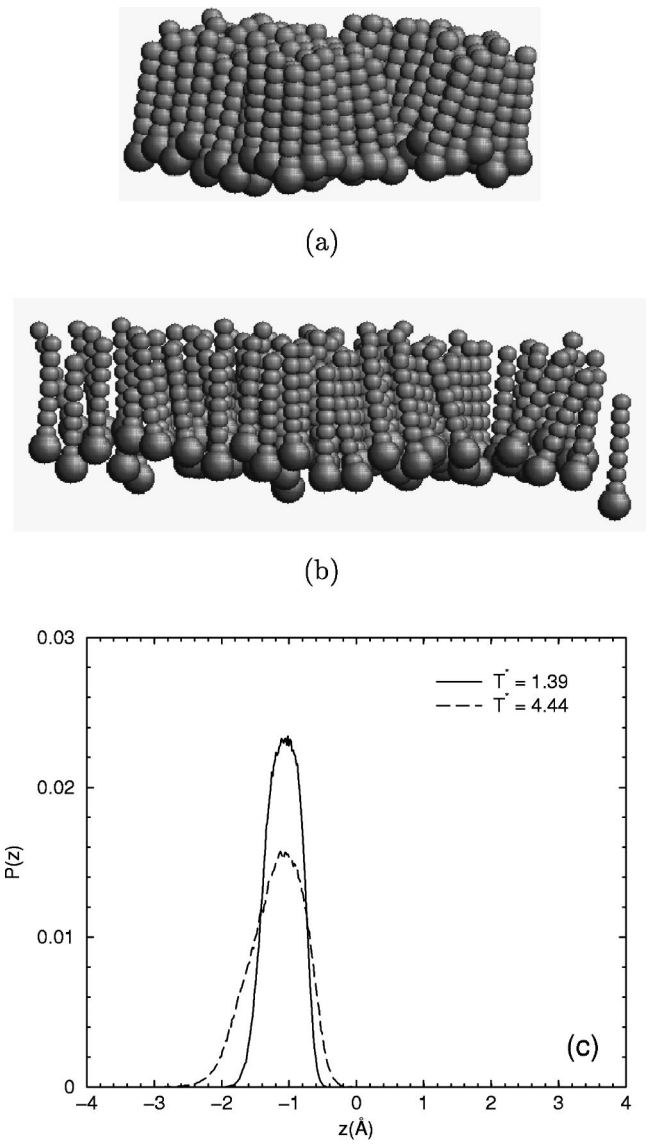

FIG. 10. Equilibrium configurations using the FL model at $\rho^* = 1.12$, $n_t = 7$, for $\sigma_{hh} = 1.20\sigma_{tt}$: (a) $T^* = 1.39$, (b) $T^* = 4.44$, (c) corresponding z displacement probability distributions.

most noticeable effects due to the water subphase, is the substantial reduction in the tilt angle. Since the head groups are allowed to form a staggered structure, the tails do not have to tilt as far in order to maintain an optimal packing. Although the monolayer enters a liquidlike state at lower temperatures than found with the hard surface model, the monolayer still remains stable and does not buckle to form multilayered structures or enter a gaseous phase, as found with the (9-3) model. Thus, from our preliminary studies with the FL model we find that it provides a more realistic description of the surfactant-water interactions than the 9-3 model and is capable of replicating staggering behavior such as found in experiments [20,21] as well as in molecular-dynamics studies [24] of more complex microsopic models.

V. CONCLUSIONS

Using a simplified microscopic model for Langmuir monolayers, we have demonstrated that the model exhibits tilting transitions from uniformly tilted to untilted structures with increasing temperature. At low temperatures, uniformly tilted phases exist in one of the NN, NNN, or I directions. Depending on head-tail diameter mismatch, there can also occur tilting transitions between different tilted phases. These results concur with both experimental work and other simulation studies [1,2,17,18].

To compare the phase behavior of our model system and the generic phase diagram for Langmuir monolayers, we first studied the effects on tilting transitions due to variations in

TABLE I. The width and mean z displacement of the interface formed by head groups at the water surface using the FL model at $T^* = 1.39$.

	$\sigma_{hh} = 1.10\sigma_{tt}$	$\sigma_{hh} = 1.20\sigma_{tt}$
Mean z displacement (Å)	−1.037	−1.088
Width of interface (Å)	0.212	0.484

the density. It was shown by ground-state analysis in Ref. [9] that increasing the area, for fixed head diameter or bondlength, resulted in transitions between tilted phases. At higher temperatures, we also find a dependence of the tilting transition temperature T_c on area or density; in particular, T_c increases with increase in density. We noted that there was an intermediate regime where there did not appear to be a strong correlation between density and T_c. Since all of the tilted phases corresponded to tilting in the NNN direction, we compared our phase diagram with that for Langmuir monolayers of alcohols or esters, as recently determined by experiment [10,11], and surmised that this could correspond to the $L_2'/\mathrm{Ov}-L_1$ coexistence region. Although such coexistence between condensed and liquid phases has been predicted to not occur for rigid rods [13], it is clear that we find a transition from a tilted (NNN)-condensed phase to an untilted-liquid phase. However, a larger range of densities needs to be examined in order to confirm the existence of an $L_2'/\mathrm{Ov}-L_1$ transition in the present model and obtain a more complete phase diagram.

The main emphasis of this paper has been the investigation of the effects of head-tail diameter mismatch on tilting transitions at higher temperatures. It was found that as this mismatch increases, the critical tilting transition temperature T_c decreases. Although the ground-state analysis of Ref. [9] indicated that an increase in the mismatch between head and tail diameters favors a tilted state at low temperatures, which is an energetic effect, at higher temperatures the increase in mismatch favors an untilted state, an entropic effect. With greater mismatch between head and tail diameters, there is more available volume for the surfactant tails to reorient. The resultant increase in the orientational entropy tends to drive down T_c. Hence, we see that the effects of head-tail diameter mismatch on the tilting behavior of the model system is determined by a competition between energetically and entropically driven processes.

Although for the longer tail lengths of $n_t=7$, we still observed a trend towards decreased T_c for increased head-tail diameter mismatch, the transitions were shifted to higher temperatures compared with $n_t=4$, as anticipated from experiment [1–3]. That is, the longer chains tend to stabilize the tilted phases and induce more pronounced tilt ordering. Furthermore, the increased chain length tended to diminish differences in T_c due to this mismatch, i.e., the effect of the head-tail diameter is less prominent for longer tail lengths.

We also find low-temperature tilt-ordering transitions between different tilted phases. For the shorter tails of length $n_t=4$, the resulting phases are short lived and are immediately followed, at slightly higher temperatures, by transitions to untilted disordered states. It is quite possible that, at greater densities, the tilted phases resulting from low-temperature tilt-ordering transitions could be stabilized. Since the present simulations have been performed in the NAT ensemble, we expect that there is frustration of the system, which inhibits observing true first-order transitions associated with the changes in area and lattice distortion that should accompany changes in tilt direction. By fixing the area and, more importantly, the shape of the simulation cell, our calculations suppress the expected first-order transition and make it difficult to establish true tilt ordering. What is observed, instead, is a composite structure composed of both NN and NNN tilting. However, since the area is constant, these phases are not in equilibrium with each other (i.e., they are at different pressures). At low temperatures, this constraint results in negative surface pressures indicative of the metastability of the system. To alleviate this problem, one should execute simulations in the NΠT ensemble, as recently considered by Stadler *et al.* [5,6].

Although the majority of the work presented here was performed using the HS model, in which the water subphase was replaced by a hard attractive surface, we have also utilized the (9-3) potential model to account for surfactant-water interactions. However, using this model, it was found that the monolayer would buckle, akin to the phenomenon termed ''collapse,'' forming bilayer or multilayered structures at temperatures and densities where one would expect to find the liquid phase for a Langmuir monolayer. The sudden jump to a gas phase, and the apparent lack of a liquidlike phase, can be attributed to the ''softness'' of the potential, which allows the head groups to leave the water surface with only a small penalty in energy but with a substantial increase in entropy. Thus, it is favorable for the molecules to leave the surface even at moderate temperatures.

We have shown that a more realistic model to characterize the water subphase is the FL model developed by Karaborni and Toxvaerd [14,15]. An advantageous feature of this model is that the head groups are allowed to penetrate into the water subphase. In combination with this property, the tail-water interactions are not infinitely repulsive and, thus, allow for some mixing of the tail groups with water. It appears that these features are responsible for producing the staggering of head groups across the air-water interface observed in our simulations, an effect which is certainly seen in experiment [20,21], and a substantial decrease in the mean tilt angle. At low temperatures, we find that there are small fluctuations of the head groups across the interface. As the temperature is increased, the magnitude of these fluctuations increases and, in the disordered phase, leads to the presence of surface waves. In our preliminary studies with this model, we find (as with the HS model) that increased head-tail mismatch results in a decrease in the transition temperature T_c from the tilted to untilted phase. Additionally, it appears that this mismatch tends to accentuate the disordering of the monolayer due to the presence of the water subphase. The destabilization of the monolayer for larger head diameters, where the tilting is in the NN direction, implies that the L_2-L_1 phase boundary for acids and acetates should move to *lower* temperatures relative to the $L_2'/\mathrm{Ov}-L_1$ phase boundary for esters and alcohols. This feature has yet to be examined in experimental studies.

A natural extension to our Monte Carlo work would be to consider semiflexible chains and study the role that chain ordering and packing have on tilting transitions. Additionally, we have seen that to avoid some of the artifacts due to periodic boundary effects present in NAT simulations, it would be preferrable to utilize the NΠT ensemble. Such research has been performed by Stadler *et al.* [5] and Stadler and Schmid [6], who have examined the phase diagrams cor-

responding to surfactants with head diameters of $\sigma_{hh}=1.1$ and $\sigma_{tt}=1.2$. As such, it would be more fruitful for us to focus on other unresolved issues related to details of the phase diagram for Langmuir monolayers, which have yet to be addressed. In particular, we have begun more detailed studies of the coupling between the effective head-group-size and head-group-water interactions in terms of the role they play in determining tilt ordering.

[1] C. M. Knobler and R. C. Desai, Annu. Rev. Phys. Chem. **43**, 207 (1992).
[2] V. M. Kaganer, H. Möhwald, and P. Dutta, Rev. Mod. Phys. **71**, 779 (1999).
[3] A. M. Bibo and I. R. Peterson, Adv. Mater. **2**, 309 (1990).
[4] M. K. Durbin, A. Malik, A. G. Richter, R. Ghaskadvi, T. Gog, and P. Dutta, J. Chem. Phys. **106**, 8216 (1997).
[5] C. Stadler, H. Lange, and F. Schmid, Phys. Rev. E **59**, 4248 (1999).
[6] C. Stadler and F. Schmid, J. Chem. Phys. **110**, 9697 (1999).
[7] C. Lautz, T. M. Fischer, and J. Kildea, J. Chem. Phys. **106**, 7448 (1997).
[8] F. Schmid and H. Lange, J. Chem. Phys. **106**, 3757 (1997).
[9] S. B. Opps, B. G. Nickel, C. G. Gray, and D. E. Sullivan, J. Chem. Phys. **113**, 339 (2000).
[10] M. C. Shih, M. K. Durbin, A. Malik, P. Zschack, and P. Dutta, J. Chem. Phys. **101**, 9132 (1994).
[11] E. Teer, C. M. Knobler, C. Lautz, S. Wurlitzer, J. Kildae, and T. M. Fischer, J. Chem. Phys. **106**, 1913 (1997).
[12] S. Ramos and R. Castillo, J. Chem. Phys. **110**, 7021 (1999).
[13] F. Schmid, Phys. Rev. E **55**, 5774 (1997).
[14] S. Karaborni and S. Toxvaerd, J. Chem. Phys. **97**, 5876 (1992).
[15] S. Karaborni and S. Toxvaerd, J. Chem. Phys. **96**, 5505 (1992).
[16] M. Scheringer, R. Hilfer, and K. Binder, J. Chem. Phys. **96**, 2269 (1992).
[17] F. M. Haas, R. Hilfer, and K. Binder, J. Chem. Phys. **102**, 2960 (1995).
[18] F. M. Haas, R. Hilfer, and K. Binder, J. Chem. Phys. **100**, 15 290 (1996).
[19] J. Harris and S. A. Rice, J. Chem. Phys. **89**, 5898 (1988).
[20] J. R. Lu, Z. X. Li, R. K. Thomas, E. J. Staples, I. Tucker, and J. Penfold, J. Phys. Chem. **97**, 8012 (1993).
[21] J. R. Lu, M. Hromadova, R. K. Thomas, and J. Penfold, Langmuir **9**, 2417 (1993).
[22] P. Belohorec and B. G. Nickel (unpublished); P. Belohorec, Ph.D. thesis, University of Guelph, 1997 (unpublished).
[23] S. B. Opps, Ph.D. thesis, University of Guelph, 1999 (unpublished).
[24] J. Böcker, M. Schlenkrich, P. Bopp, and J. Brickmann, J. Phys. Chem. **96**, 9915 (1992).